

Original Article

Refined Computer Model of Auxiliary Induction Motor of Electric Locomotive Powered by Autonomous Voltage Inverter

Mikhail Pustovetov

Mechanical Engineering Technology Department, Technological Institute (Branch) of Don State Technical University in the City of Azov, Russia.

mgsn2006@yandex.ru

Received: 28 June 2023; Revised: 21 July 2023; Accepted: 28 August 2023; Published: 03 October 2023;

Abstract - The article's research object is to improve the accuracy of computer simulation of a variable frequency auxiliary electric drive of an AC electric locomotive and, more precisely, the current of the stator phase of an auxiliary induction motor when powered by an autonomous voltage inverter. The research topic of the article is the substantiation of additions to the computer model of a 3-phase induction motor, which allows taking into account the influence on the values of the leakage inductances of phases of the skin effect, as well as the saturation of the magnetic circuit from the leakage fluxes. As a research method, computer simulation using OrCAD software was chosen based on the introduction in the model of experimentally obtained oscillograms of phase voltages of an auxiliary induction motor. The results of computer simulation of the steady state with various initial data are presented and analytically compared with the data obtained experimentally. Based on a comparison of a number of characteristics of the operating mode of the electric motor (phase current, torque, rotational speed), it was concluded that it is advisable to use an augmented computer model to increase the reliability of the simulation.

Keywords - Auxiliary induction motor phase current, Leakage inductance, Magnetic circuit saturation, Skin effect, Variable frequency electric drive.

1. Introduction

Induction Motors (IM), due to the simplicity of their design, proven manufacturing technology, and reliability in operation, are perhaps the most common electric machines in the world [1]. A Variable Frequency electric Drive (VFD) with 3-phase IM is used on electric rolling stock both as a traction [2] and auxiliary [3, 4]. In view of the relative simplicity of the mechanisms of the auxiliary electric drive and the small range of regulation of the operating speeds for the auxiliary electric drive, the VFD with scalar speed control based on a two-level Autonomous Voltage Inverter (AVI) has become widespread [4 - 6]. For example, as part of the PSN-169 auxiliary converter onboard an EP200 Russian AC mainline electric locomotive, the AVI is a load of an active power factor corrector [6, 7].

For the analysis and synthesis of operating modes of IM as part of electric drives, it is customary to use computer simulation [8 - 10]. This information technology allows you to reduce product development time, consider many different options, recognize unsuccessful technical solutions and choose acceptable ways to correct them.



It has been noticed that when simulating processes in IM as part of the VFD, there are some inconsistencies between the experimental current curve and the calculated one: the simulation gives a discrepancy with the experiment regarding instantaneous current values. This can be seen, for example, from the illustrations given in [9, 11] for the phase current obtained as a result of the experiment and the calculated curves of the phase current of the auxiliary 3-phase IM AZhV250M2RUKhL2 fan drive (a two-pole electric machine for power supply from the AVI, rated power 110 kW, cast aluminium squirrel-cage rotor, random stator winding made of round copper wire; the parameters and characteristics of this IM are given in [9]). Compared to the one obtained as a result of computer simulation, the experimental current rises and falls faster when the phase voltage is switched and has a slightly larger amplitude.

The probable reason for the “greater mobility” of the current recorded in the experiments is the neglect in mathematical and computer models of IM [9 - 11] of the saturation of the magnetic circuit along the leakage paths, that is, the values of the stator and rotor leakage inductances that are different from the actual ones. Similar observations and conclusions can be drawn from comparing the IM phase current curves obtained as a result of the experiment and computer simulation presented in [12] and [13]. However, a similar difference in the behavior of currents when powered by AVI is also inherent in significantly more complex mathematical models of IM [14], as can be seen from the graphs of the current of the NTA-1200 traction IM presented in the book [14].

When using the simulation results to select AVI semiconductor devices by current, it is recommended to multiply the amplitude of the current obtained as a result of the simulation by a factor equal to 1.3 - 1.35 in order to take into account the “greater mobility” of the current recorded in the experiments, according to compared with the current obtained in the simulation [9 - 11]. The calculated current curve can be obtained using the harmonic analysis method based on the T-shaped equivalent circuit of the IM phase [1] (Figure 1, borrowed from [11]).

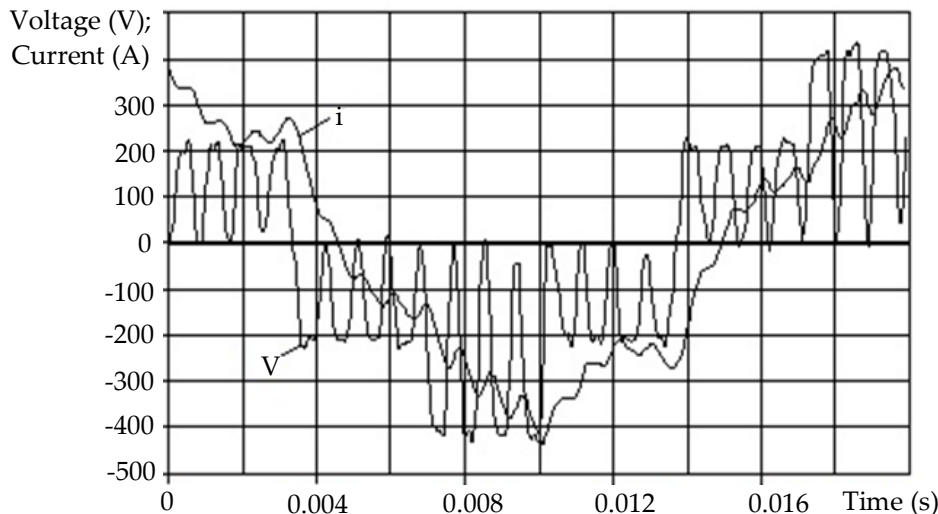


Fig. 1 Calculated voltage and current curves of the AM AZhV250M2RUKhL2 phase when powered by a frequency converter at $f_1=48.4$ Hz, obtained using the harmonic analysis method. The voltage is synthesized from odd harmonics of orders not multiple of three from the 1st to the 97th, obtained from the expansion of the experimental curve of the phase voltage in a Fourier series

The method of harmonic analysis is described in detail in [15, 16]. In [17], the method was refined: corrections were made to the previously used software for calculating the electromagnetic torque. A feature of the harmonic analysis method is the separate consideration for each time harmonic of the influence of the current displacement effect on the resistances and inductances of the equivalent circuit using the expressions described in [18]. The saturation of the magnetic circuit from the main flux is given by a fixed value of the saturation coefficient. The

saturation of the magnetic circuit with leakage fluxes is not taken into account. The disadvantage of the harmonic analysis method is its development and applicability only to steady-state operating modes of IM. Moreover, the rotor slip value is set as one of the initial conditions for calculation, remaining unchanged without undergoing any fluctuations (the rotor motion equation is not in the process of solution), which, strictly speaking, is an idealized approach for most IM operation modes when powered by AVI.

The group of rows 10 in Table of Appendix presents calculation data achieved using the harmonic analysis method compared with results of the experiment for the steady state mode of a motor-fan based on IM AZhV250M2RUKhL2, powered by AVI, which is a part of PSN-169, at a frequency of the fundamental harmonic $f_1=48.4$ Hz. We have a Root Mean Square Error (RMSE) of 9.91% regarding the experimental curve (row 1 in Table of Appendix). All RMSE values in the Table of Appendix are normalized to the highest instantaneous value of the current obtained in the experiment for the considered time interval.

2. Formulation of the Problem

The works [9, 10] describe in detail the mathematical and computer models of a 3-phase IM in three-phase stator reference frames, developed by the author, based on the T-shaped equivalent circuit of the IM and solving a system of Ordinary Differential Equations (ODE) and algebraic equations [1], including the equation of motion of the rotor. Unlike the method of harmonic analysis, this model allows us to consider both transient and steady processes in IM. The model also makes it possible to consider the phenomenon of saturation of the magnetic circuit with the main magnetic flux coupled simultaneously with the magnetic circuits of the stator and rotor through the air gap. The module of the instantaneous value of the amplitude of the representing vector of the flux linkage of the mutual induction is calculated through the orthogonal projections of the vector in the same way described in [8]. The structures and techniques tested in the computer model [9, 10] implemented using the OrCAD software [19, 20] have been successfully used to develop IM models [21] in the Matlab environment [22], which contain useful developments that make it possible to take into account the effect of inter-turn short circuits in the stator winding on the mode of operation of an electric machine.

Returning to the comparison of the computer model [9, 10] with the harmonic analysis method, we note that, according to [9, 10], the influence of the skin effect on resistances and inductances is not considered. The saturation of the magnetic circuit with leakage fluxes is also not considered.

Questions arise: 1) How do the assumptions made in the model [9, 10] affect the correspondence of the simulated current curve of the stator phase of the IM to the experimentally obtained current curve when powered by the AVI? 2) How can the model [9, 10] be supplemented to take into account the influence of the skin effect and saturation from leakage magnetic fluxes on the leakage inductances? In [10, 12 - 14], the voltage signals applied to the phases of computer models of IM are formed using one or another computer model of the AVI; that is, they are inevitably idealized and somewhat differ in shape from the voltage oscillograms recorded during the experiment. For example, in Figure 1, the IM phase voltage curve, used as an input signal in the calculations, is synthesized based on a truncated Fourier series, from which harmonic components of orders higher than 97 are discarded, which is visually perceived as a smoothed form of voltage pulses compared to the expected a set of pulses, the shape of which is close to rectangular. But the use of ideal trapezoidal voltage pulses with very steep slopes in simulation is also a deviation from the truth: the duration of the slopes depends on the specific type of semiconductor switches used, and the shape of the trapezoid is actually curvilinear since it is distorted by the influence of both the switching processes of the switches themselves and the influence of parasitic elements of the converter installation, random processes of electromagnetic interaction with other equipment. These circumstances make it possible to justify the divergence of the IM phase currents obtained as a simulation result and experiment. The logic is simple: since there are differences in the input signals (voltages on the IM phases) during simulation and experiment, they will lead to differences in the output signals (currents of the IM phases).

In order to exclude the influence of inaccuracy in the reproduction by the computer model of the AVI of the details of the voltage form recorded during the experiments on the result of the current simulation, we will apply voltage oscillograms obtained experimentally to the phases of the computer model of the IM type AZhV250M2RUKHL2 (this approach has already been used by the author by means of another software and described in [11]). Oscillograms of voltages and currents of IM type AZhV250M2RUKhL2 were obtained experimentally by specialists of JSC VEINII (Novocherkassk, Russia) during tests of PSN-169 and published in [6].

The answer to the first of the questions posed is contained in row group 2 of Table of Appendix: for the phase current curve obtained as a result of computer simulation, we have RMSE = 9.58%. Let us try to make additions to the computer model of IM [9, 10] to reduce the RMSE value.

3. Accounting for Saturation from Leakage Magnetic Fluxes

As is known, in electrical machines, in addition to the main magnetic flux, there are leakage magnetic fluxes [1]. With the level of detail inherent in the above-mentioned computer models of IM [1, 9, 10, 21], we should talk about the leakage magnetic fluxes of each phase of the stator and rotor windings. Let us clarify that, for example, the leakage magnetic flux of phase B of the stator is coupled exclusively to the stator (does not penetrate through the air gap into the rotor) and exclusively to phase B of the stator winding of the IM. Suppose the nonlinearity of the magnetization curve from the main magnetic flux determines the variability of the value of the main inductance in the IM equivalent circuit. In that case, the nonlinearity of the magnetization curve from leakage magnetic fluxes determines the variability of the values of the leakage inductances of the phases of the stator and rotor windings of the IM. In other words, the phase leakage inductance of the IM winding depends on the magnitude of the current flowing through this winding. In [23], a case is described when, for one of the types of IM, the saturation of the magnetic system with leakage fluxes had a decisive influence on the characteristics of the operating modes of the electric machine. That is, taking this phenomenon into account may be important to ensure the adequacy of simulating processes in IM.

Usually (also in the case of AM type AZhV250M2RUKhL2), the dependencies of leakage inductances on current are unknown. According to the recommendation [23], the nonlinearity that characterizes the change in the leakage inductance should cover the operating modes of the AM from idle to locked rotor. For IM type AZhV250M2RUKhL2, the values of the reactances of the stator and rotor in the starting mode at a sinusoidal voltage are known, which are respectively 98.2% and 81.1% of the values at the rated mode, that is, these are the values at $s=1$. Agreeing with [23] that it is difficult to separate the effect of saturation phenomena and the skin effect on the leakage inductance, we pay attention to the fact that both in the locked-rotor mode and in the idle mode, a current of the same frequency flows through the stator leakage inductance. This implies the conclusion that, in any case in the stator, the decrease in the leakage reactance (and in direct proportion to the leakage inductance) is due to large values of starting currents but not the current frequency (not the phenomenon of the skin effect). For uniformity, we extend the same approach to the reduced leakage reactance of the rotor.

Figure 2 shows the form of non-linearities of the stator and rotor leakage inductances, respectively, adopted for simulation. We will use first curves 1 and 2.

The author in [9, 24] provides a detailed description of the mathematical and computer models of the saturable electric choke. The same approach is proposed to be used to take into account the saturation of the leakage inductances of the windings of the stator and rotor phases by magnetic fluxes in a computer model of a 3-phase IM. In Figure 3, we can see a graphical representation of the computer model of phase A of the windings of the stator and rotor of the IM according to [9, 10] (original version). In Figures 3 - 5, as sensors and for inputting signals in the IM model, elements of the type VSCV, VSCL, and CSCV are used. In these abbreviations: S - source; V - voltage; C - current; CV - controlled by voltage; CC - controlled by current. For example, VSCL is a voltage

source controlled by current. In Figures 4 and 5 (a variant of the circuit [25] supplemented to take into account saturation from leakage magnetic fluxes), the ABS block performs the operation of taking the signal absolute value. The Table block is a table in which the leakage inductance values (per unit) are given as a function of the instantaneous stator current. A block in the form of a rectangle, having the designation "1.0" inside, is a source of the constant voltage of 1.0 V. Resistors have large values, for example, 10 MΩ. Practically without affecting the numerical results of the simulation, they stabilize the solution (simulation) by maintaining the current circuit (the physical sense - is the way for leakage current), which is especially important when discretely changing the resistance of the IM power supply circuits, for example, when powered by a semiconductor frequency converter or when phase failure happens.

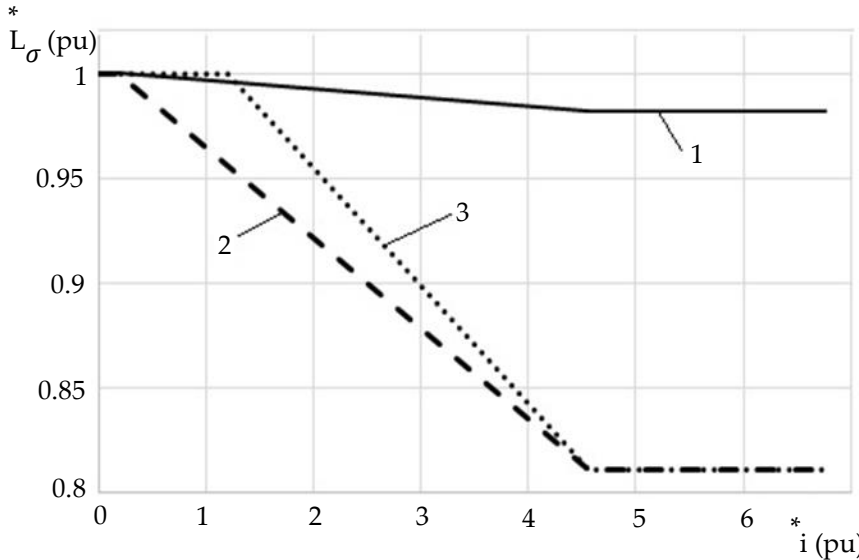


Fig. 2 The non-linearities of leakage inductances of the stator and rotor of IM AZhV250M2RUKhL2 adopted for simulating per units:
curve 1 - $L_{\sigma 1}^*(i)$; curve 2 – the initial version of $L'_{\sigma 2}^*(i)$; curve 3 - the final version of $L'_{\sigma 2}^*(i)$

Note that resistive elements of this purpose are used by other developers of computer models of electrical devices [26]. Similar to Figure 4, the saturation of the magnetic circuit with leakage fluxes in the phases of the IM rotor is taken into account in this way: having added the lower part of Figure 3, we get Figure 5. According to the 2nd Kirchhoff law for phase α of the stator and rotor (reduced to the stator [9, 10]) of the IM, taking into account [9, 24], equations (1) and (2) can be written, respectively (notation according to [9, 24] and Figures 3 - 5)

$$v_{sa} + \Delta L_{\sigma sa}(i_{sa}) \cdot \frac{di_{sa}}{dt} = r_{sa} \cdot i_{sa} + L_{\sigma sa} \cdot \frac{di_{sa}}{dt} + v_{0\alpha} \quad (1)$$

$$v_{ra} + \Delta L_{\sigma ra}(i_{ra}) \cdot \frac{di_{ra}}{dt} = e_{0\alpha} - e_{rot\alpha} - L_{\sigma ra} \cdot \frac{di_{ra}}{dt} - r_{ra} \cdot i_{ra} \quad (2)$$

In equations (1) and (2), respectively, for the stator and rotor $\Delta L_{\sigma}(i)$ - the instantaneous value of the difference between the unsaturated and saturated values of the leakage inductance (for Figures 4 and 5), i.e. between a constant value L_{σ} , which does not take into account the effect of saturation from leakage fluxes (relative value $L_{\sigma}=1$ pu), and a variable value $L_{\sigma sat}(i)$ depending on the instant value of the current, which takes into account the effect of saturation from leak-age fluxes (relative value $L_{\sigma sat}(i) \leq 1$ pu).

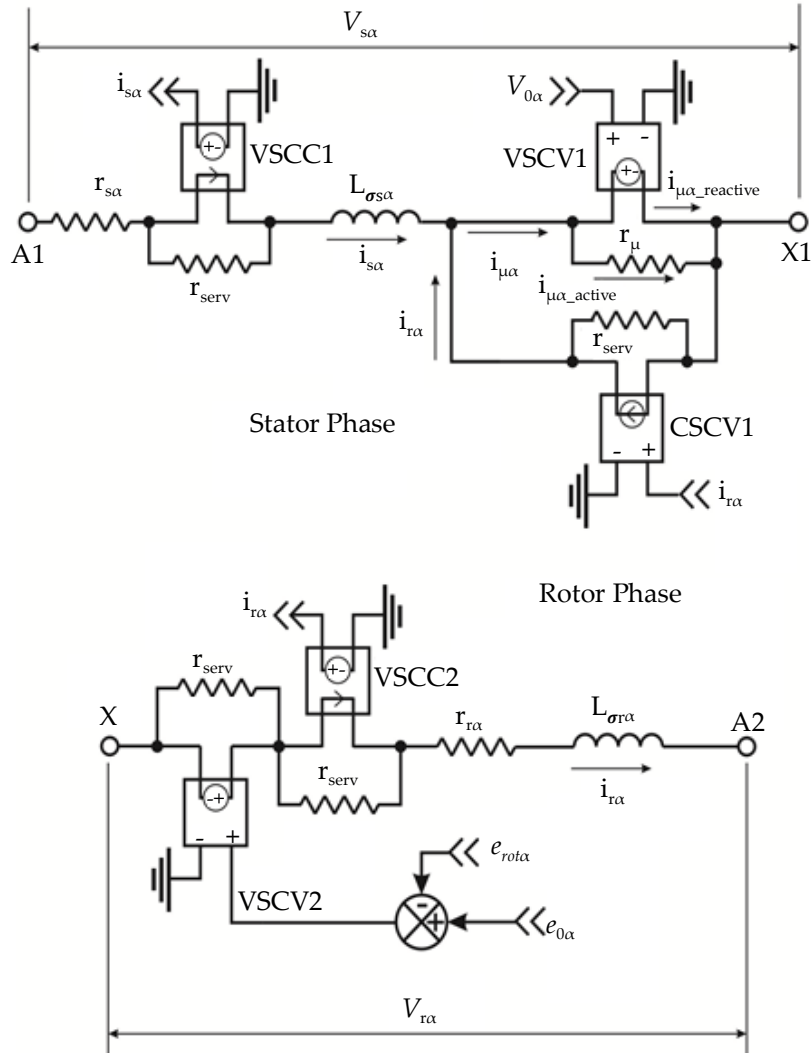


Fig. 3 Graphical representation of the original (excluding saturation by leakage fluxes) computer model of phase A of the stator and rotor windings of a 3-phase IM according to [9]

The Table block in Figure 4 implements a nonlinear dependence of the stator leakage inductance on the stator phase current according to curve 1 in Figure 2. The Table block in Figure 5 implements a non-linear dependence of the rotor leakage inductance on the rotor phase current according to curve 2 in Figure 2. The parameters of the rotor phase and its current are reduced to the stator. For simplicity, in the denominator of the gain of the amplifier block before the Table block in Figure 5, you can use the current value $I_{1\text{rated}}$ as the base value. EMF $\Delta L_{\sigma\alpha}(i_{ra}) \cdot \frac{di_{ra}}{dt}$ is introduced into the electrical circuit of the stator phase by means of VSCV3 (see Figure 4), and

EMF is introduced into the electrical circuit of the rotor phase by means of VSCV6 (see Figure 5). For other phases, the equations are similar to (1) and (2).

According to the group of rows 3 in Table of Appendix, for the phase current curve simulated taking into account the decrease in leakage inductance due to saturation from the leakage magnetic fluxes, we have RMSE = 10.14%, which, unexpectedly, indicates an increase in the difference between the current curves obtained as a result of computer simulation and experiment. On the contrary, the author expected the convergence of the shapes of the curves. We will analyze the reason for the discrepancy between the expectation and the fact a little later.

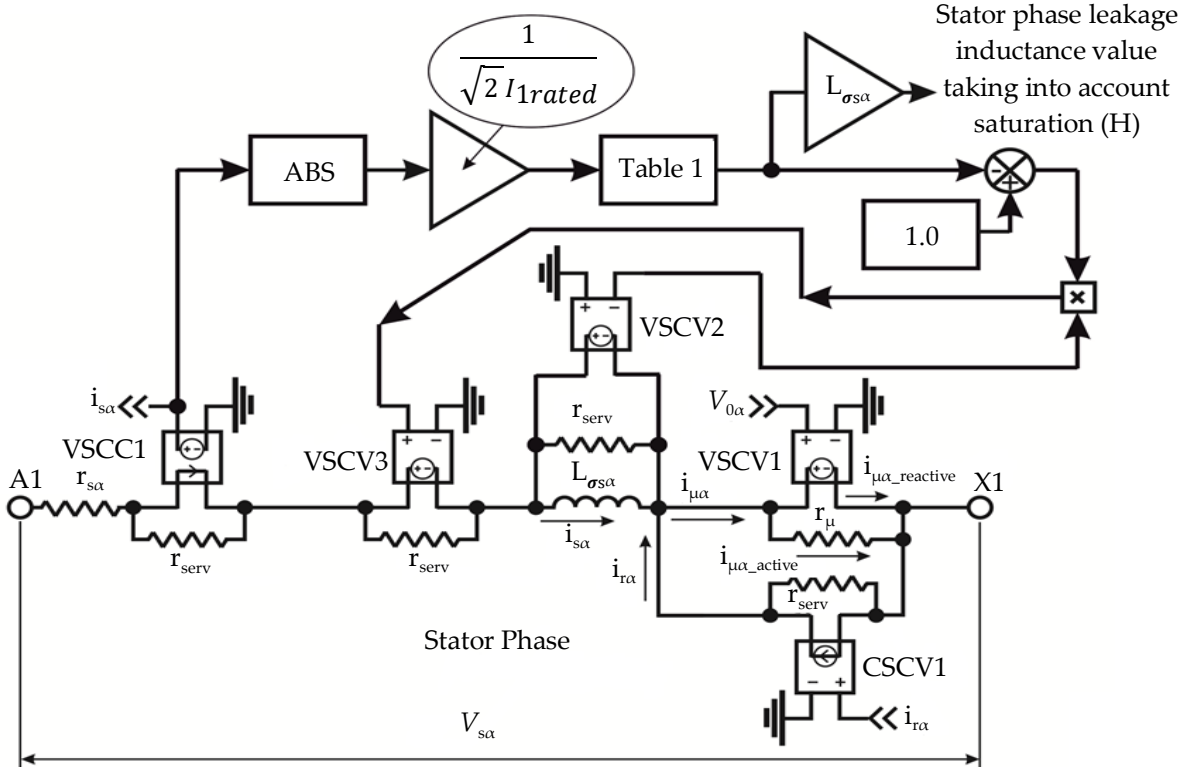


Fig. 4 Graphical representation of the modified (taking into account the saturation by the stator leakage flux) computer model of phase A of the stator winding of the IM

4. Accounting for the Influence of the Skin Effect on the Leakage Inductance

As can be seen in Figure 1, the output voltage of the AVI is non-sinusoidal poly-harmonic. Due to the switching of voltage pulses, the current has clearly pronounced ripples, the shape of which is close to triangular. The frequency of these ripples exceeds the frequency of the main current harmonic. At elevated frequencies, it is reasonable to expect manifestations of the skin effect, including one that reduces the value of leakage inductances [27]. As a rule, taking into account the skin effect, which depends on the current frequency, in the mathematical modelling of IM is replaced by taking into account its dependence on slip s [28, 29].

But in this way, it is possible to consider the action of the skin effect only in the rotor during transient processes of rotational speed. In our case, the simulation results compare for a steady state (quasi-static, strictly speaking) when the speed fluctuations are cyclic and insignificant in magnitude. In mathematical models of IM based on ODE systems, there is no signal corresponding to the frequency of current or voltage. But in an explicit form, there are rates of change of currents - these are the first derivatives of currents with respect to time $\frac{di_i}{dt}$

i'_i . It is proposed to use them instead of frequencies f_1 and f_2 to take into account the influence of the skin effect.

Note that the replacement of frequency values by the first derivative of induction with respect to time is used in calculating the components of iron losses at non-sinusoidal voltage [30 - 32]. In fairness, you can get the value f_1 in the IM model from the rotational speed setting signal or by analyzing the period of the set phase voltage, but this gives only the frequency of the fundamental harmonic, so it will not help when taking into account the influence of the skin effect at poly-harmonic currents.

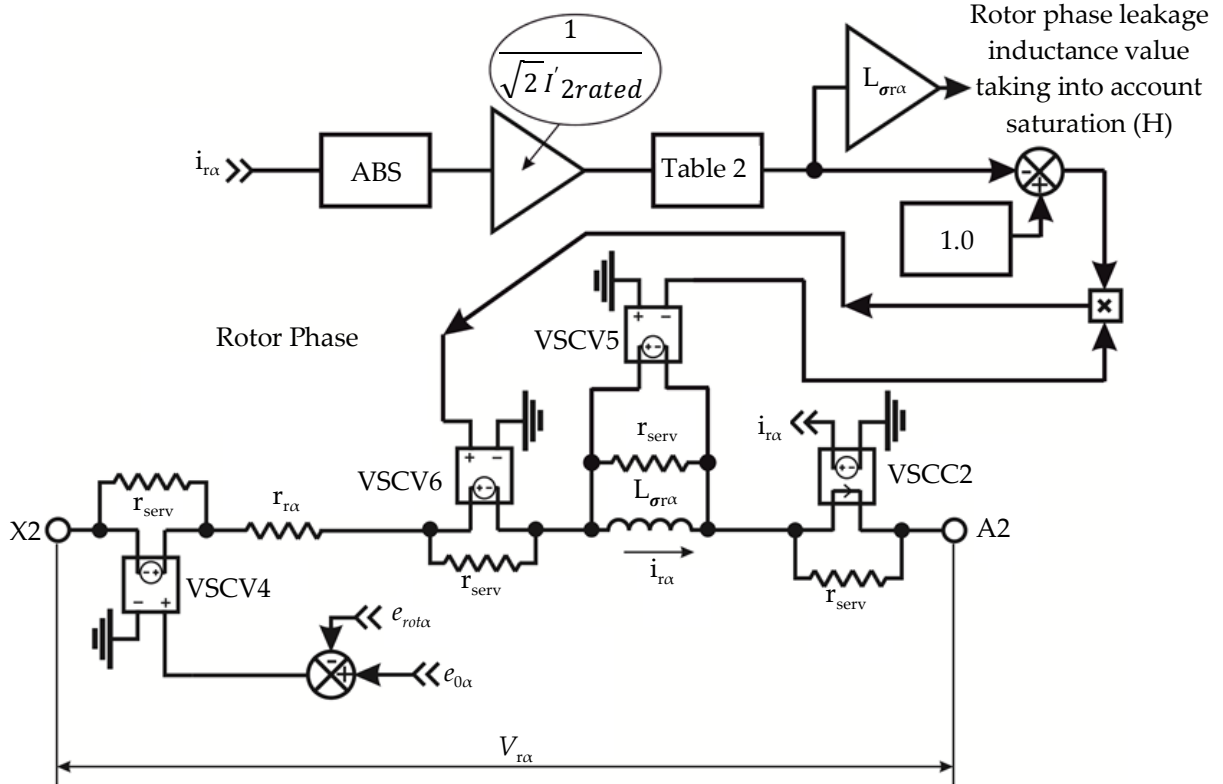


Fig. 5 Graphical representation of the modified (taking into account the saturation by the rotor leakage flux) computer model of phase A of the rotor winding of the IM (reduced to stator)

In [33], an approximation of the experimentally obtained dependences of leakage inductances on the frequency of the current for an IM with a rated power from 2.2 kW to 160 kW is presented by the expression $L_o(f) = K_L \cdot f^{(-0.16)}$, where $K_L = \text{const}$. For example, due to the influence of the skin effect, the leakage inductance at a frequency of 20 kHz will be 2.6 times less than at 50 Hz. For IM AZhV250M2RUKhL2, all parameters are known for a sinusoidal current with a frequency of 50 Hz. Therefore, as a basic value $\frac{di}{dt}$, we can use the

amplitude value of the current of the stator phase $\sqrt{2} \cdot 197 \text{ A}$, achieved in a quarter of the period $\frac{1}{4 \cdot f_{rated}} = \frac{1}{4 \cdot 50} = \frac{0.02}{4} = 0.005 \text{ s}$. It is necessary to take into account the features of the physics of the processes in the

rotor: despite the fact that in the mathematical model, the parameters of the rotor are reduced to the stator, and in the equivalent circuit, the current frequency in the rotor circuit is the same as in the stator, naturally the current frequency in the rotor $f_2 = s \cdot f_1$. Therefore, we multiply for the rotor phase $\frac{di'_2}{dt}$ by the instantaneous slip value s .

In addition, we will limit the maximum value of the ratio

$$\left(\frac{di}{dt} \right) \left/ \left(\frac{\sqrt{2} \cdot I_{rated}}{1/(4 \cdot f_{rated})} \right) \right. = 1$$

Figures 6 and 7 show the computer models of the stator and rotor of IM's phases supplemented with allowance for the influence of the skin effect. In Figures 6 and 7, LIMIT blocks limit the output signal between the values 0 and 1 inclusive. The PWR(-0.16) blocks raise the absolute value of the input signal to the power of -0.16.

According to the data in row group 6 in Table of Appendix, for the phase current curve obtained as a simulation result, while taking into account the decrease in leakage inductances due to saturation from leakage magnetic fluxes and the action of the skin effect, we have RMSE = 9.45%, which does not satisfy us, since it almost does not differ from the RMSE value in the group of rows 2 in Table of Appendix.

Now, for Figures 6 and 7 in equations (1) and (2), respectively, for the stator and rotor, it is necessary to take into account $\Delta L_\sigma(i, f)$ - the instantaneous value of the difference between the values of the leakage inductance without the influence of saturation and the skin effect and with such an influence.

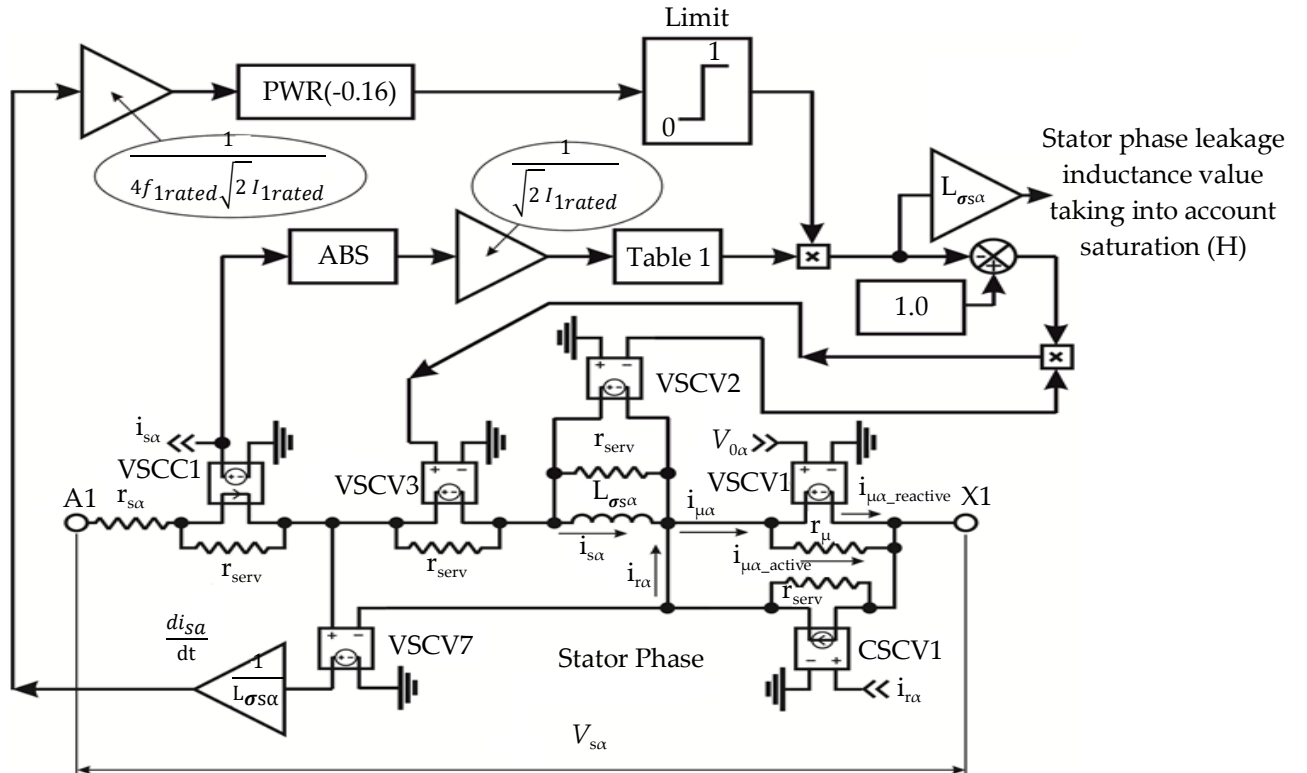


Fig. 6 Graphical representation of the modified (taking into account the saturation by the stator leakage flux and the influence of the skin effect on the leakage inductance) computer model of phase A of the stator winding of the IM

Computer models are good because they can turn off the influence of certain physical effects, which is difficult, if not impossible, in real objects. We turn off the effect of saturation from leakage fluxes on the leakage inductance of the rotor. The result for this case is given in row group 7 in Table of Appendix: RMSE = 8.18%, which is clearly better. Taking into account the results in row groups 4 and 8 in Table of Appendix, it can be concluded that in the considered mode of operation of the IM AZhV250M2RUKhL2, there is no decrease in the leakage inductance of the rotor, caused by saturation of the steel with magnetic leakage fluxes. But in transient modes, when high currents occur, such saturation is quite possible. Therefore, it is not advisable to completely disable this effect in the model. Let us change the dependence of the leakage inductance of the rotor on the current in such a way that saturation does not have an effect up to the current $1.2 \cdot \sqrt{2} \cdot I_{\text{rated}}$. This corresponds to using curve 3 instead of curve 2 (see Figure 2). The simulation results for such a configuration (line group 9 in Table of Appendix and Figure 8) give RMSE = 8.04%. An attempt to enhance the influence of the skin effect on the leakage inductance by using the expression $L_\sigma(f) = K_L \cdot f^{(-0.5)}$ in the model did not lead to convergence of the current curves obtained as a result of computer simulation and experiment: RMSE = 8.13% (comparison of row group 5 with row group 4 in Table of Appendix ceteris paribus).

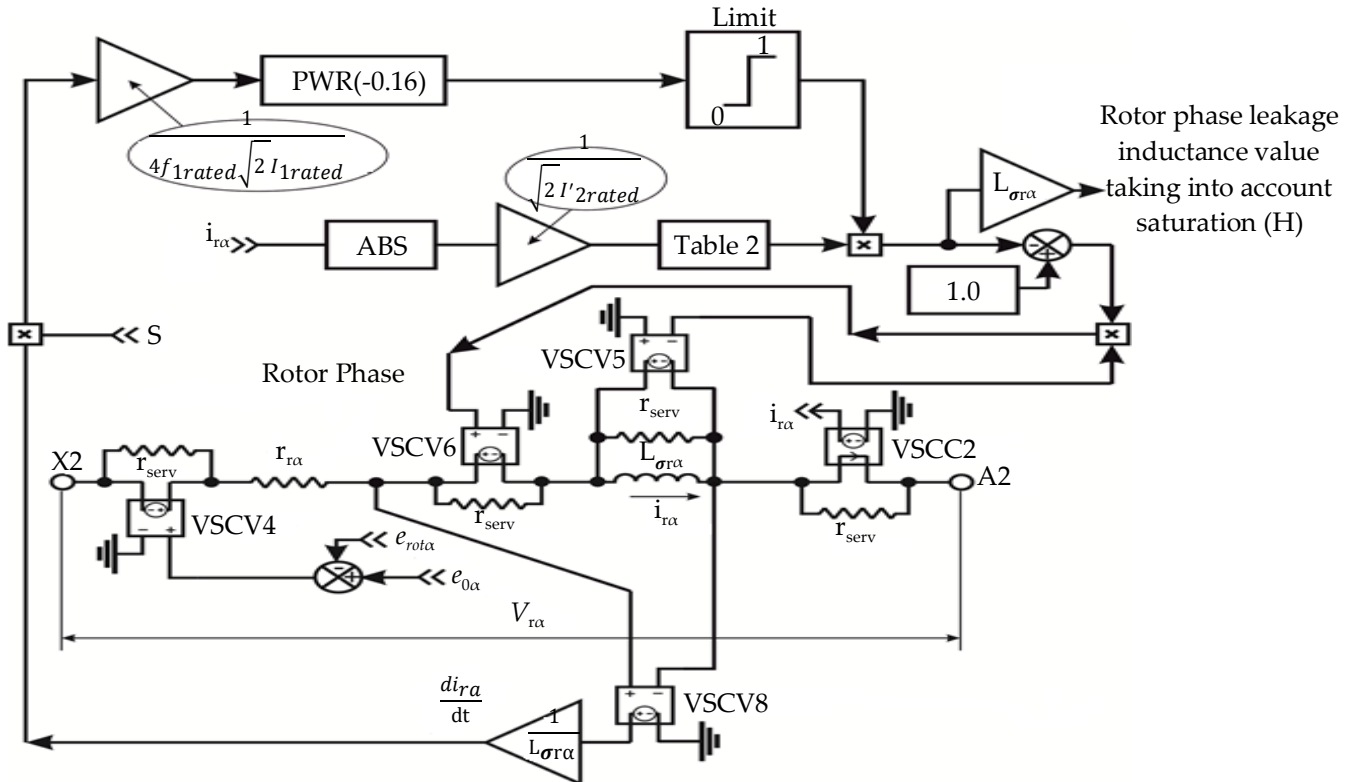


Fig. 7 Graphical representation of the modified (taking into account the saturation by the rotor leakage flux and the influence of the skin effect on the leakage inductance) computer model of phase A of the rotor winding of the IM

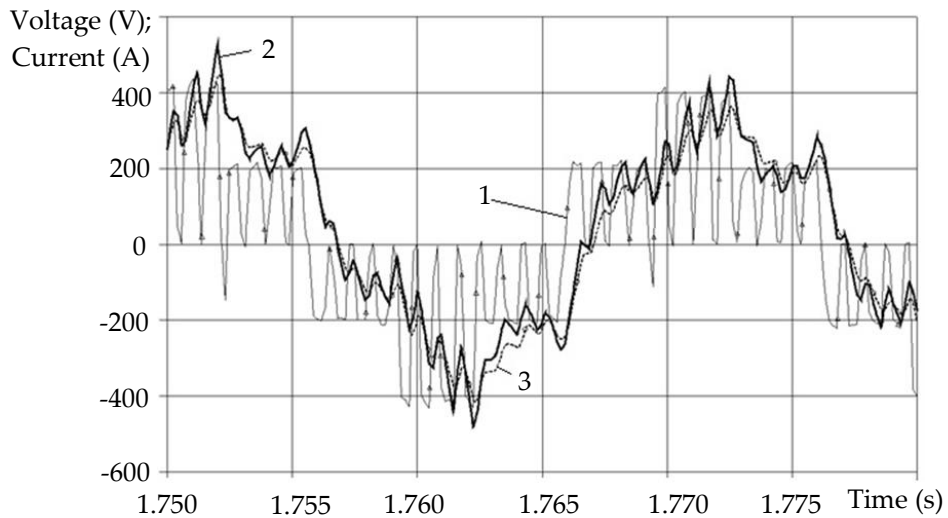


Fig. 8 Illustration of the nature of the difference in the phase current curves of the IM type AZhV250M2RUKhL2, obtained experimentally and as a result of computer simulation, when powered by a frequency converter at $f_1=48.4$ Hz, taking into account that the magnetic circuit is saturated not only with the main flux but also with stator and rotor leakage fluxes, as well as taking into account the influence of the skin effect on the leakage inductances of the stator and rotor: curve 1 is the stator phase voltage obtained experimentally (used as an input signal during the computer simulation); curve 2 – stator phase current obtained experimentally; curve 3 - stator phase current obtained as a result of computer simulation

Figure 9 illustrates the influence of various factors on the relative value of the stator phase leakage inductance $L_{\sigma 1}$ (to the simulation results shown in Figure 8): curve 1 is the effect of stator leakage flux saturation; curve 2 is the influence of the skin effect. Without taking into account the influences, we have the $L_{\sigma 1} = 1 \text{ pu}$. With the adopted structure and limitations of the IM model, the influence of the same factors on the relative value of the leakage inductance of the rotor phase is much weaker: the skin effect does not appear at all, and the decrease in inductance due to saturation of the rotor leakage flux is insignificant (not lower than 98%) and has a pulsed character only for certain highest current peaks (see Figure 10).

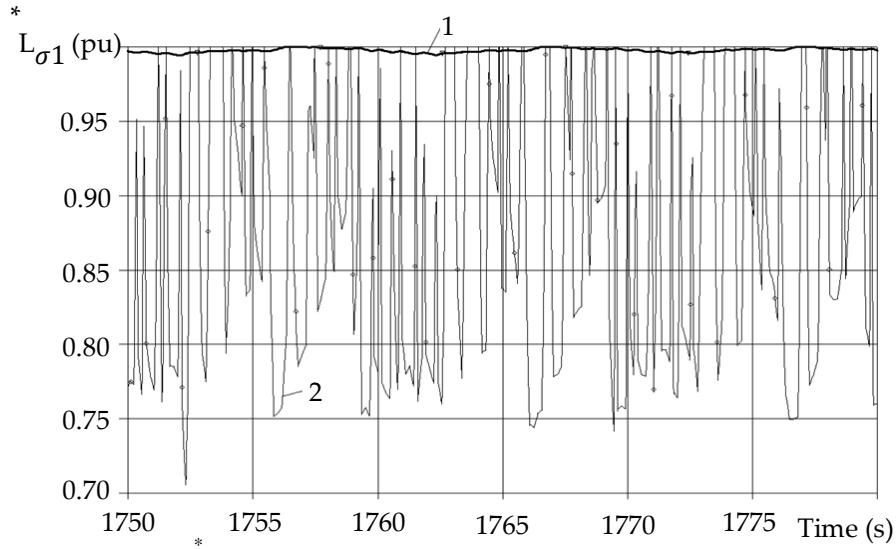


Fig. 9 Influence on the relative value $L_{\sigma 1}$ of various factors (to the simulation results shown in figure 8): curve 1 - the influence of the saturation by the stator leakage flux; curve 2 - the influence of the skin effect

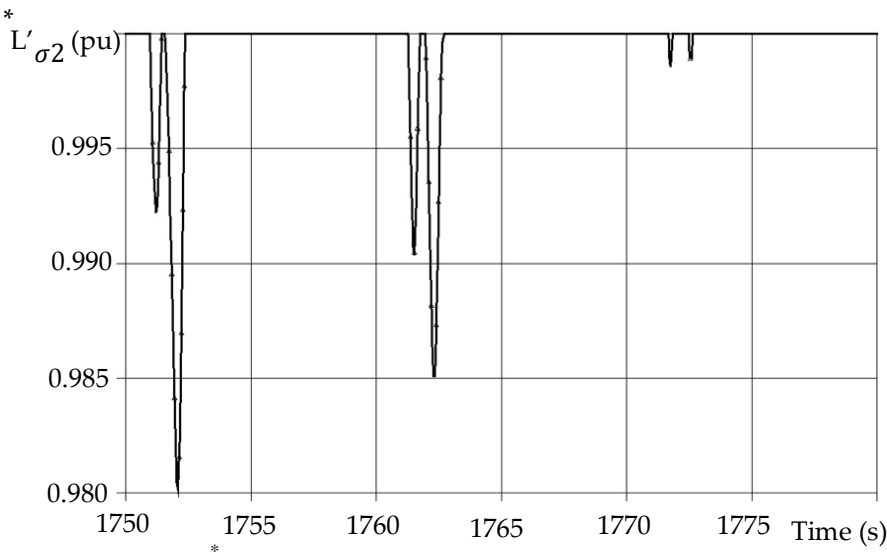


Fig. 10 Influence on the relative value $L'_{\sigma 2}$ of saturation from the leakage magnetic flux of the rotor (to the simulation results shown in figure 8)

5. Conclusion

In general, the current obtained as a result of computer simulation continues to demonstrate "less mobility" compared to the experimentally obtained one with all the signs indicated at the beginning of the article. At the same time, the use of additions in the computer model that takes into account the influence of the skin effect on the leakage inductance and the saturation of the magnetic circuit with leakage fluxes (see Figures 6 and 7) gave a positive result in the form of a decrease in the RMSE of the simulated stator phase current curve from that obtained experimentally. For the considered mode of operation of IM type AZhv250M2RUKhL2, the greatest positive impact was made by taking into account the action of the skin effect on the leakage inductance of the stator winding. An additional advantage of the proposed additions to the computer model of IM is that, being introduced into the model structure, they (their influence) can be partially or completely "turned off" without removing the additions from the model structure. It is very important that the additions introduced into the computer model of the IM did not worsen the correspondence of the fundamental characteristics (the effective value of the fundamental harmonic of the phase current, the average values of the rotation frequency and torque) obtained as a result of the simulation, to the experimental ones.

References

- [1] Theodore Wildi, *Electrical Machines, Drives and Power Systems*, 6th ed., Upper Saddle River, USA, Pearson Prentice Hall, 2005. [\[Google Scholar\]](#) [\[Publisher Link\]](#)
- [2] Mikhail Pustovetov, "The Determination of Mode of Load by the Adhesion for Locomotives with Induction Traction Motors," *DS Journal of Digital Science and Technology*, vol. 2, no. 2, pp. 23-31, 2023. [\[CrossRef\]](#) [\[Google Scholar\]](#) [\[Publisher Link\]](#)
- [3] Saurabh Kamble et al., "Investigation of Harmonics Present in Three-Phase Auxiliary Converter used in the Locomotives of Indian Railways," *Journal of the Institution of Engineers (India): Series B*, vol. 101, pp. 101–105, 2020. [\[CrossRef\]](#) [\[Google Scholar\]](#) [\[Publisher Link\]](#)
- [4] Shri Rupesh Kumar, Ed., *Traction Rolling Stock: Three Phase Technology*, Indian Railways, Institute of Electrical Engineering, 2010. [Online] Available: <https://irieen.indianrailways.gov.in/uploads/files/1302581203548-Three%20phase%20Technology-291010.pdf>
- [5] N.P. Tishkin et al., "Energy Saving in the Power Supply Systems of Auxiliary Electrical Machines of the Ermak Series AC Electric Locomotive Due to the Use of SHPVM-250-U2," *Bulletin of VEINII (Vestnik VELNII)*, vol. 1 no. 63, pp. 63–74, 2012.
- [6] I.V. Pekhotskiy et al., "Power Converter for Controlled Auxiliary Electric Drive of AC Electric Locomotive EP200," *Electrical Locomotives Building (Elektrovozstroenie)*, vol. 44, pp. 249–256, 2002.
- [7] M. Yu. Pustovetov, "Modeling of a Two-Circuit System of Subordinate Control of the Coordinates of the Active Power Factor Corrector of the Auxiliary Electric Drive of an Electric Locomotive," *Bulletin of the Scientific Research Institute of Railway Transport, Russian Railway Science Journal*, vol. 81, no. 2, pp. 125-133, 2022. [\[CrossRef\]](#) [\[Google Scholar\]](#) [\[Publisher Link\]](#)
- [8] Sergey Goolak et al., "Improving a Model of the Induction Traction Motor Operation Involving Non-Symmetric Stator Windings," *Eastern-European Journal of Enterprise Technologies*, vol. 4, no. 8 (112), pp. 45–58, 2021. [\[CrossRef\]](#) [\[Google Scholar\]](#) [\[Publisher Link\]](#)
- [9] M. Pustovetov, *Computer Modeling of Induction Motors and Transformers. Examples of Interaction with Power Electronic Converters*, Saarbrucken, Germany: LAP LAMBERT Academic Publishing, 2013. [\[Google Scholar\]](#)
- [10] Mikhali Pustovetov, "Induction Electrical Machine Simulation at Three-Phase Stator Reference Frame: Approach and Results," *Applied Electromechanical Devices and Machines for Electric Mobility Solutions*, pp. 63-78, 2020. [\[CrossRef\]](#) [\[Google Scholar\]](#) [\[Publisher Link\]](#)
- [11] I.V. Pekhotskiy et al., "Simulation of Processes in an Induction Motor Powered by Controlled Inverter Output Voltage," *Electrical Locomotives Building (Elektrovozstroenie)*, vol. 44, pp. 184–193, 2002.
- [12] Hadeed A. Sher et al., "Theoretical and Experimental Analysis of Inverter Fed Induction Motor System Under DC link capacitor Failure," *Journal of King Saud University – Engineering Sciences*, vol. 29, pp. 103–111, 2017. [\[CrossRef\]](#) [\[Google Scholar\]](#) [\[Publisher Link\]](#)
- [13] K. Reddy Sudharshana et al., "Simulation and Experimental Validation of Common Mode Voltage in Induction Motor Driven by Inverter using Arduino Microcontroller," *Proceedings of the World Congress on Engineering WCE 2017*, vol. 1, 2017. [\[Google Scholar\]](#) [\[Publisher Link\]](#)

- [14] Zarifyan Alexander Aleksandrovich et al., "Dynamic Processes in the Asynchronous Traction Drive of Main Electric Locators," *Scientific Electronic Library LLC*, 2006. [[Google Scholar](#)] [[Publisher Link](#)]
- [15] I.I. Talya, I.L. Targonsky, and A.L. Lozanovsky, "Calculation of the Characteristics of an Induction Electric Motor at Non-Sinusoidal Voltage," *Electrical Locomotives Building (Elektrovozostroenie)*, vol. 34, pp. 66-76, 1994.
- [16] I.I. Talya, et al., "Electromagnetic Torque of an Induction Electric Motor at Non-Sinusoidal Voltage," *Electrical Locomotives Building (Elektrovozostroenie)*, vol. 35, pp. 106-115, 1995
- [17] I.I. Talya, and M. Yu. Pustovetov, "On the Ripple of the Electromagnetic Torque of an Induction Traction Motor in the Starting Mode," *Bulletin of Higher Educational Institutions. Electromechanics*, no. 4, pp. 34-37, 1998.
- [18] J. Lameraner, and M. Stafl, *Eddy Currents*, London, UK: Ilife, 1968.
- [19] John Keown, *OrCAD PSpice and Circuit Analysis*, 4th edition, Prentice Hall, 2000. [[Google Scholar](#)] [[Publisher Link](#)]
- [20] Muhammad H. Rashid, *SPICE for Power Electronics and Electric Power*, 3rd edition, Boca Raton, USA: CRC Press, 2012. [[Publisher Link](#)]
- [21] Sergey Goolak et al., "Analysis of Control Methods for the Traction Drive of an Alternating Current Electric Locomotive," *Symmetry*, vol. 14, no. 1, p. 150, 2022. [[CrossRef](#)] [[Google Scholar](#)] [[Publisher Link](#)]
- [22] Eklas Hossain, *MATLAB and Simulink Crash Course for Engineers*, Springer, 2022. [[CrossRef](#)] [[Google Scholar](#)] [[Publisher Link](#)]
- [23] G. A. Sipailov, and A. V. Loos, *Mathematical Modelling of Electrical Machines (for Analog Computers)*, Moscow, Russia: Vysshaya Shkola, 1980.
- [24] Mikhail Pustovetov, "An Inductive Coil Simulation," *International Journal of Power Systems*, vol. 6, pp. 90-93, 2021. [[Google Scholar](#)] [[Publisher Link](#)]
- [25] Mikhail Pustovetov, "Modification of the Computer Model of the 3-Phase Asynchronous Motor to Ensure the Accounting of Magnetic Saturation by Scattering Currents," *Instrumental Bibliometric National*, vol. 1, pp. 496-499, 2023. [[Google Scholar](#)] [[Publisher Link](#)]
- [26] Sergey E. Zirka, Yuriy I. Moroz, and Cesare M. Arturi, "Accounting for the Influence of the Tank Walls in the Zero-Sequence Topological Model of a Three-Phase, Three-Limb Transformer," *IEEE Transactions on Power Delivery*, vol. 29, no. 5, pp. 2172-2179, 2014. [[CrossRef](#)] [[Google Scholar](#)] [[Publisher Link](#)]
- [27] P.R. Wilson, and R. Wilcock, "Frequency Dependent Model of Leakage Inductance for Magnetic Components," *Advanced Electromagnetics*, vol. 1, no. 3, pp. 99-106, 2012. [[CrossRef](#)] [[Google Scholar](#)] [[Publisher Link](#)]
- [28] Zakari Maddi, and Djamel Aouzellag, "Dynamic Modelling of Induction Motor Squirrel Cage for Different Shapes of Rotor Deep Bars with Estimation of the Skin Effect," *Progress in Electromagnetics Research*, vol. 59, pp. 147-160, 2017. [[CrossRef](#)] [[Google Scholar](#)] [[Publisher Link](#)]
- [29] J. Maksimkina, "The Research of the Processes of the Squirrel-Cage Induction Motor's Direct Start-up in the Setting of the Rotor's Variable Parameters," *Power and Electrical Engineering*, vol. 30, pp. 53-58, 2012. [[Google Scholar](#)] [[Publisher Link](#)]
- [30] Helmut Pfützner, Georgi Shilyashki, and Emanuel Huber, "Calculated Versus Measured Iron Losses and Instantaneous Magnetization Power Functions of Electrical Steel," *Electrical Engineering*, vol. 104, pp. 2449-2455, 2022. [[CrossRef](#)] [[Google Scholar](#)] [[Publisher Link](#)]
- [31] Jan Rens, Lode Vandenbossche, and Ophélie Dorez, "Iron Loss Modelling of Electrical Traction Motors for Improved Prediction of Higher Harmonic Losses," *World Electric Vehicle Journal*, vol. 11, no. 1, p. 1-14, 2020. [[CrossRef](#)] [[Google Scholar](#)] [[Publisher Link](#)]
- [32] M. Torrent et al., "Method for Estimating Core Losses in Switched Reluctance Motors," *European Transactions on Electrical Power*, vol. 21, no. 1, pp. 757-771, 2011. [[CrossRef](#)] [[Google Scholar](#)] [[Publisher Link](#)]
- [33] D.W. Novotny, "Frequency Dependence of Time Harmonic Losses in Induction Machines," *Proceeding International Conference on Electric Machine*, vol. 90, pp. 233-238, 1990. [[Google Scholar](#)]

Appendix

Table 1. Comparative characteristics of the operating mode of the motor fan based on IM AZhV250M2RUKhL2, fed from the AVI, obtained by different methods

#	Characteristics of the Analyzed Mode	Frequency of the 1st Harmonic of the Supply Voltage (Hz)	RMS Value of the 1st Harmonic of the Stator Current (A)	Average Value of Rotational Speed (rpm)	Average Value of Shaft Torque (Nm)	Maximum Calculated Value of Electromagnetic Torque (Nm)	Minimum Calculated Value of Electromagnetic Torque (Nm)	Ripple Coefficient of Electromagnetic Torque (%)	RMSE (%) of the Calculated Curve of the Phase Current from the Experimental
1	Experiment	48.4	235.7	2869.5	360.0	Data are absent			-
For all the variants of simulation based on the equations given in [9, 10]: 1) saturation of the magnetic system with the main magnetic flux is taken into account; 2) the influence of the skin effect on the resistance of the windings is not taken into account; 3) voltage curves obtained experimentally (by means of sensors and an analog-to-digital converter) are applied to the phases of the IM model									
2									
2	Computer simulation	48.4	242.3	2868.6	346.7	449.8	261.9	27.1	9.58
	Without taking into account the influence on the leakage inductances of the stator and rotor of the skin effect and saturation of the magnetic circuit								
3									
3	Computer simulation	48.4	242.8	2868.7	346.8	448.7	264.1	26.6	10.14
	Taking into account the influence on the leakage inductances of the stator and rotor saturation of the magnetic circuit. The influence on the inductance of the skin effect is not taken into account.								
4									
4	Computer simulation	48.4	236.1	2872.6	350.1	476.5	232.4	34.9	8.09
	Taking into account the influence on the stator leakage inductance of: 1) saturation of the magnetic circuit and 2) skin effect as a function of the stator current frequency $f_1^{0.16}$. The influence on the rotor leakage inductance of the saturation of the magnetic circuit and the skin effect is not taken into account.								
5									
5	Computer simulation	48.4	232.4	2872.6	350.1	476.5	232.4	34.9	8.13

	Taking into account the influence on the stator leakage inductance of: 1) saturation of the magnetic circuit and 2) skin effect as a function of the stator current frequency $f_1^{-0.5}$. The influence on the rotor leakage inductance of the saturation of the magnetic circuit and the skin effect is not taken into account.								
	Calculation error, %	-1.390	0.108	-2.756	-	-	-	-	
	Computer simulation	48.4	225.9	2875.1	349.0	466.8	246.8	31.5	9.45
6	Taking into account the influence on the stator leakage inductance of: 1) saturation of the magnetic circuit and 2) skin effect as a function of the stator current frequency $f_1^{-0.16}$.								
	Taking into account the influence on the rotor leakage inductance of: 1) saturation of the magnetic circuit and 2) skin effect as a function of the rotor current frequency $f_2=(s.f_1)^{-0.16}$.								
	Calculation error, %	-4.186	0.195	-3.050	-	-	-	-	
	Computer simulation	48.4	237.6	2871.3	348.1	460.8	251.4	30.1	8.18
7	Taking into account the influence on the stator leakage inductance of: 1) saturation of the magnetic circuit and 2) skin effect as a function of the stator current frequency $f_1^{-0.16}$.								
	Taking into account the influence on the rotor leakage inductance of skin effect as a function of the rotor current frequency $f_2=(s.f_1)^{-0.16}$. The influence of the saturation of the magnetic circuit on the rotor leakage inductance is not taken into account.								
	calculation error, %	0.785	0.063	-3.304	-	-	-	-	
	Computer simulation	48.4	242.2	2868.7	347.2	452.8	259.8	27.8	9.21
8	Taking into account the influence on the leakage inductances of the stator and rotor saturation of the magnetic circuit. There is no effect of saturation on the leakage inductance of the rotor up to the current value $1.2 \sqrt{2} I_{\text{rated}}$.								
	Calculation error, %	2.741	0.028	-3.546	-	-	-	-	
	Computer simulation	48.4	237.3	2871.3	347.7	460.0	247.5	30.5	8.04
9	Taking into account the influence on the stator leakage inductance of: 1) saturation of the magnetic circuit and 2) skin effect as a function of the stator current frequency $f_1^{-0.16}$.								
	Taking into account the influence on the rotor leakage inductance of: 1) saturation of the magnetic circuit and 2) skin effect as a function of the rotor current frequency $f_2=(s.f_1)^{-0.16}$. There is no effect of saturation on the leakage inductance of the rotor up to the current value $1.2 \sqrt{2} I_{\text{rated}}$. See Figure 8.								
	calculation error, %	0.688	0.063	-3.415	-	-	-	-	

	Calculation by the method of harmonic analysis	48.4	245.0	2845.9	365.0	441.0	302.0	19.0	9.91
10	When calculating according to the method of harmonic analysis [15-17]: 1) the saturation of the magnetic system with the main magnetic flux is taken into account; 2) the influence of the skin effect on the resistance of the rotor winding is taken into account; 3) the phase voltage is synthesized from odd harmonics of orders of non-multiple three from the 1st to the 97th, obtained from the expansion of the experimental curve of the phase voltage; 4) the influence of the skin effect on the leakage inductances of the stator and rotor in the slot parts of the windings is taken into account; 5) the influence of the skin effect on the resistance of the stator winding is not taken into account; 6) the effect on the leakage inductance of the stator and rotor of the saturation of the magnetic circuit is not taken into account								
	Calculation error, %	3.946	0.822	1.389	-	-	-	-	-